THE EFFECT OF PERFORATION ON THE RADIATION EFFICIENCY OF VIBRATING PLATES

FJ Fahy Institute of Sound and Vibration Research
DJ Thompson University of Southampton
Southampton SO17 1BJ
United Kingdom

1 INTRODUCTION

One means of reducing the sound radiated by the plate-like structures of vibrating machinery components and ancillary structures such as safety guard enclosures and product collection hoppers is to construct them from perforated sheets. However, there appears to be little quantitative guidance relating to the design and effectiveness of this noise reduction measure.

A theoretical model is first presented of radiation by plane bending waves propagating in an unbounded, uniformly perforated, plate. It is then shown how this model is applied to calculate the radiation efficiency of the modes of a simply-supported, rectangular, perforated plate. To do so it has to be assumed that the plate is mounted in a similarly perforated coplanar baffle. This model can be extended to allow for the situation in which the plate and the baffle have different specific acoustic impedances, e.g. a perforated plate mounted in an unperforated baffle. However, such an approach is computationally extremely intensive. As a preliminary, and less computationally demanding, problem, a theoretical model of radiation by a perforated strip piston vibrating in a coplanar baffle of different specific acoustic impedance is developed. Examples are presented of the results derived from the various models. The results of an experimental programme to determine the radiation efficiency of a series of unbaffled, perforated, rectangular plates are also presented. Conclusions relevant to noise control practice are drawn.

2 RADIATION BY PLANE BENDING WAVES IN AN UNBOUNDED PERFORATED PLATE

The acoustic impedance of a single circular hole of radius r in an otherwise rigid plane baffle of thickness t, in the range of frequency ω such that $\omega r/c = kr$ <<1, is inertial and given by[1]

$$Z_h = j\frac{\omega\rho_0}{2r}\left(1+\frac{2t}{\pi r}\right) \tag{1}$$

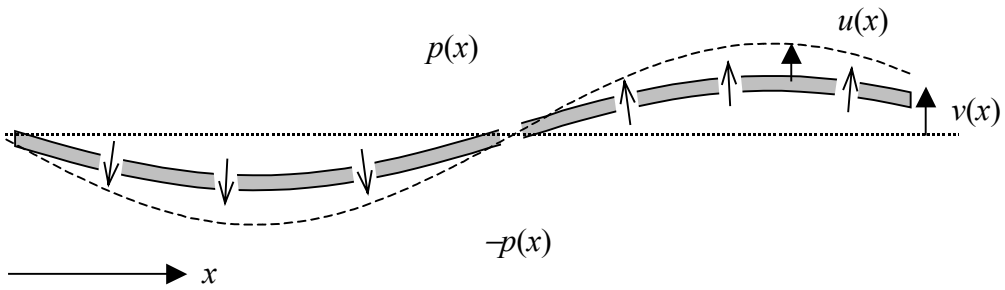

Figure 1. A bending wave on an infinite perforated plate.

In order to apply this to a perforate with a uniform array of holes, Figure 1, it is assumed that the acoustic near-field associated with flow through each hole is sufficiently weak not to interact with flow through adjacent holes. Then the array can be represented by an equivalent, *continuously distributed*, uniform specific acoustic impedance, given by[2]

$$z_h = j\frac{\omega\rho_0 S}{2r}\left(1+\frac{2t}{\pi r}\right) = j\rho_0 c\frac{kS}{2r}\left(1+\frac{2t}{\pi r}\right) = j\rho_0 ch \tag{2}$$

where S (<< k^2) is the area per hole and the non-dimensional specific acoustic impedance h has been introduced. For thin plates the term in brackets tends to 1. It should be noted that, in addition to its dependence upon purely geometric quantities, h is proportional to frequency. Hence, for a given perforate geometry, it varies widely in magnitude over the frequency range of interest in noise control. The physical reason is that the counter-flow through the holes, which reduces radiation, is controlled by the inertial reaction of the fluid in the vicinity of the holes: this increases with frequency. Also, if a hole has a viscous acoustic resistance R = Re{pressure difference/volume velocity}, the equivalent specific acoustic resistance of an array of holes is RS, which must be added to z_h, making it complex instead of purely imaginary. Thus, jh should be replaced by $jh+RS/\rho_0 c$.

A plane, harmonic, bending wave of frequency ω and wavenumber k_x is assumed to propagate in the x-direction in an unbounded uniform (unperforated) plate lying in a horizontal plane. The normal velocity of the plate $v(x)$ (assumed to be positive upwards) is spatially harmonic and may be expressed as

$$v(x) = v(k_x)\exp(-jk_x x) \tag{3}$$

where $v(k_x)$ is the complex amplitude of v. The plate velocity generates a complex acoustic pressure amplitude $p_0(k_x)$ on the upper surface given by[3]

$$\frac{p_0(k_x)}{v(k_x)} = z_a(k_x) = \frac{\rho_0 ck}{\sqrt{k^2 - k_x^{\,2}}} \qquad \text{when } k_x < k \tag{4a}$$

$$\frac{p_0(k_x)}{v(k_x)} = z_a(k_x) = j\frac{\rho_0 ck}{\sqrt{k_x^{\,2} - k^2}} \qquad \text{when } k_x > k \tag{4b}$$

where $z_a(k_x)$ is the specific acoustic radiation impedance presented to the upper surface of the plate by the fluid. The pressure on the lower surface is $-p_0(k_x)$.

In the case of a perforated plate, fluid is driven through the individual holes by the difference between the local pressures on the upper and lower surfaces of the plate. These pressures, in turn, are modified by the flow through the holes. The flow through the holes relative to the plate can be written as an equivalent, continuously distributed, upward directed, fluid particle velocity $u(x)$ (see Figure 1), which is given by

$$u(x) = -2\frac{p(x)}{z_h} \tag{5}$$

where p is the upper surface pressure that results from the combined plate velocity and equivalent continuously distributed fluid velocity through the perforate. The total continuously distributed normal velocity of combined plate and fluid motion is given by

$$w(x) = v(x) + u(x) = v(x) - 2\frac{p(x)}{z_h} \tag{6}$$

Since the plate is unbounded, and the bending wave has a unique wavenumber k_x, the equivalent continuous distribution of flow through the perforate, and any resulting surface pressure, must share the same unique wavenumber. Consequently, we may write Eq.(5) as

$$u(k_x)\exp(-jk_x x) = -2\frac{p(k_x)}{z_h}\exp(-jk_x x) \tag{7a}$$

or

$$u(k_x) = -2\frac{p(k_x)}{z_h} \tag{7b}$$

and similarly Eq.(6) as

$$w(k_x) = v(k_x) + u(k_x) = v(k_x) - 2\frac{p(k_x)}{z_h} \tag{8}$$

From Eqs.(4)

$$p(k_x) = w(k_x)z_a(k_x) = \left(v(k_x) - 2\frac{p(k_x)}{z_h}\right)z_a(k_x) \tag{9}$$

which yields

$$p(k_x) = \frac{z_h z_a(k_x)}{z_h + 2z_a(k_x)}v(k_x) \tag{10}$$

and from Eq.(5)

$$u(k_x) = \frac{-2z_a(k_x)}{z_h + 2z_a(k_x)}v(k_x) \tag{11}$$

Substitution into Eq.(8) yields the following expression for the ratio of the complex amplitudes of the combined plate and hole flow velocities to that of the plate:

$$\frac{w(k_x)}{v(k_x)} = \frac{1}{1 + 2z_a(k_x)/z_h} \tag{12}$$

As $z_a(k_x)/z_h \to 0$ (i.e. the unperforated plate), the ratio tends to unity. When $z_a(k_x)/z_h \to \infty$ (open area ratio $\to$ 100%), the ratio tends to zero (zero radiation).

The sound power per unit area radiated into the fluid above the plate is given by[3]

$$W_p(k_x) = \tfrac{1}{2}\mathrm{Re}\{p(k_x)w^*(k_x)\} = \tfrac{1}{2}\mathrm{Re}\{z_a(k_x)w(k_x)w^*(k_x)\} = \tfrac{1}{2}|w(k_x)|^2\,\mathrm{Re}\{z_a(k_x)\} \tag{13}$$

which is non-zero only when $k_x < k$ (Eq.4(a)). This condition is satisfied by free plate bending waves in an unbounded plate only above the critical frequency.

The ratio of sound power per unit area radiated by bending waves in a perforated plate to that radiated by the corresponding unperforated plate is given by

$$\frac{W_p(k_x)}{W(k_x)} = \left|\frac{w(k_x)}{v(k_x)}\right|^2 = \frac{1}{1+4\{z_a(k_x)/|z_h|\}^2} \quad \text{for } k_x < k \tag{14}$$

since z_h is imaginary. The ratio $z_a(k_x)/|z_h|$ can be written in terms of non-dimensional specific acoustic impedances as

$$\frac{z_a(k_x)}{|z_h|} = \frac{\left(1-\frac{k_x^2}{k^2}\right)^{-1/2}}{\frac{kS}{2r}\left(1+\frac{2t}{\pi r}\right)} = \frac{1}{h\left(1-\alpha^2\right)^{1/2}} \tag{15}$$

where $\alpha = k_x/k$. The insertion loss of the perforation is defined as IL(dB) = $-10\log_{10}[W_p(k_x)/W(k_x)]$. Some example results are shown in Figure 2 which shows the effect of varying h on the insertion loss for different values of k_x. For small h, the insertion loss falls at a rate of $20\log_{10}(h)$ and depends only slightly on k_x.

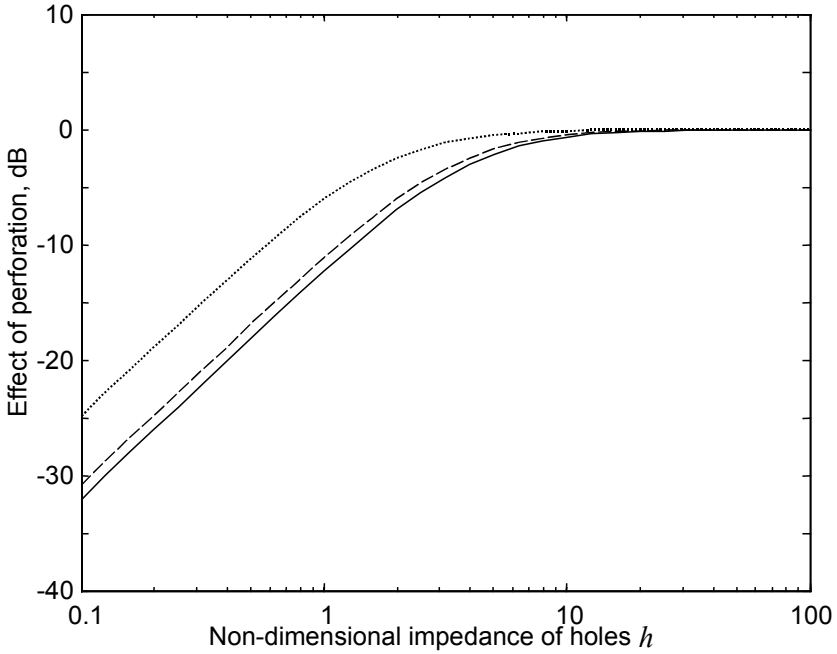

Figure 2. Effect of perforation on radiation ratio of an infinite plate as a function of non-dimensional impedance h. — $\alpha = 0$, – – – $\alpha = 0.5$, ····· $\alpha = 0.9$.

3 APPLICATION TO RADIATION BY MODES OF A RECTANGULAR PERFORATED PLATE

The sound radiation from a mode of vibration of a finite plate set in an infinite baffle can be determined by wavenumber decomposition of the spatial distribution of velocity in the mode[3]. The velocity on the baffle is zero. This can be achieved by means of the spatial Fourier transform (FT). At its resonance frequency, a mode of vibration has its largest wavenumber components at the free bending wavenumber. Nevertheless, components also exist at all wavenumbers, including those satisfying $k_x^2+k_y^2 < k$ which radiate power into the far-field, even below the critical frequency.

In order to apply the above model to a finite perforated plate, it is implied by the formulation that the plate is located in a rigid coplanar baffle *constructed of the same perforate.* Although this is a somewhat artificial configuration, the theory is next extended to model the case of a rectangular, simply-supported, perforated plate located in such a baffle. The normal velocity of the plate mode of order (p, q) is represented by

$$v(x,y,t) = v_{pq} \sin\left(\frac{p\pi x}{a}\right)\sin\left(\frac{q\pi y}{b}\right)\exp(j\omega t) \tag{16}$$

in which v_{pq} is the complex modal amplitude, a and b are the plate dimensions and ω is an *arbitrary* excitation frequency; the corresponding acoustic wavenumber $k = \omega/c$.

The relation between plate vibration and perforate flow described in Eqs.(12-14) above applies to *each* of their components of equal wavenumber. This analytical approach offers a simple and rapid means of computation of the radiation efficiency, together with a clear separation of radiating and non-radiating spectral components. The spatial distribution of normal velocity of an individual mode (as represented by Eq.(16)) is decomposed into a continuous spectrum of spatially harmonic, travelling plane wave components, each having a certain complex amplitude, wavenumber and direction of travel in the x-y plane: i.e., a certain wavenumber vector. The two-dimensional spatial Fourier transform of the modal velocity distribution expressed by Eq.(15) is defined as

$$v_{pq}(k_x,k_y) = \int_0^a\int_0^b v_{pq} \sin\left(\frac{p\pi x}{a}\right)\sin\left(\frac{q\pi y}{b}\right)\exp(-j(k_x x + k_y y))dxdy \tag{17}$$

in which $v_{pq}(k_x, k_y)$ is the complex amplitude of the wavenumber vector component of which the direction of travel is at an angle $\theta = \tan^{-1}(k_y/k_x)$ to the x-axis. Integration yields the following expression for $v_{pq}(\alpha, \beta)$ as a function of the non-dimensional wavenumbers $\alpha = k_x/k$ and $\beta = k_y/k$ and of the non-dimensional plate dimensions ka and kb [3]

$$v_{pq}(\alpha,\beta) = v_{pq} A k^{-2}(\varepsilon + j\phi)(\gamma + j\eta) \tag{18}$$

where

$$A = \frac{\left(\frac{p\pi}{ka}\right)\left(\frac{q\pi}{kb}\right)}{\left[\alpha^2 - \left(\frac{p\pi}{ka}\right)^2\right]\left[\beta^2 - \left(\frac{q\pi}{kb}\right)^2\right]}$$

$\varepsilon = (-1)^p \cos(\alpha ka) - 1$, $\phi = (-1)^{p+1}\sin(\alpha ka)$, $\gamma = (-1)^q \cos(\beta kb) - 1$ and $\gamma = (-1)^{q+1}\sin(\beta kb)$

Because the wavenumber spectrum of each plate mode is continuous, the wavenumber spectra of different modes overlap. This produces radiation coupling between the modes, and between the perforate flows. However, in air it is weak, and it diminishes with increase of mode order, so that it is generally negligible with large thin plates in the frequency range of interest: it is therefore neglected here. The reactive acoustic coupling between holes is normally negligible at hole separation distances typical of practical perforates.

From Eq.(12) the ratio of square of the modulus of the complex amplitude of the combined plate and perforate flow velocities to that of the unperforated plate is

$$|X(\alpha,\beta)|^2 = \left|\frac{w_{pq}(\alpha,\beta)}{v_{pq}(\alpha,\beta)}\right|^2 = \frac{1}{1+4\{z_a(\alpha,\beta)/|z_h|\}^2} = \frac{h^2(1-\alpha^2-\beta^2)}{4+h^2(1-\alpha^2-\beta^2)} \quad \text{for } \alpha^2+\beta^2 < 1 \quad (19)$$

The equation for the sound power radiated by a mode of a perforated plate derived using the Fourier transform effectively represents the integral over the wavenumber range $-k$ to $+k$ of Eq.(13).

$$W_{pq} = \frac{\rho_0 c\,|v_{pq}|^2}{8\pi^2 k^2}\int_{-1}^{1} d\alpha \int_{-\sqrt{1-\alpha^2}}^{\sqrt{1-\alpha^2}} d\beta \left(A^2\,|X(\alpha,\beta)|^2 \frac{(\lambda^2+\mu^2)}{(1-\alpha^2-\beta^2)^{1/2}}\right) \quad (20)$$

where $\lambda = (\varepsilon\gamma - \phi\eta)$ and $\mu = (\phi\gamma + \varepsilon\eta)$. The sound power radiated by an unperforated plate is given by Eq.(20) with $|X|$ set to unity. The integrands over α and β account for the area of non-dimensional wavenumber space enclosed by a circle of unit radius centred on the origin, because only spectral components of $v_{pq}(\alpha,\beta)$ that with $\alpha^2+\beta^2 < 1$ contribute to the radiated sound power. Other components produce purely reactive near-field components.

The radiation efficiency of a mode is given by

$$\sigma_{pq} = \frac{W_{pq}}{\rho_0 c(ab)\langle\overline{v^2}\rangle} \quad (21)$$

where $\langle\overline{v^2}\rangle$ is the space-average mean square plate velocity which is equal to $|v_{pq}|^2/8$ for all modes. From Eq.(20)

$$\sigma_{pq} = \frac{1}{\pi^2(ka)(kb)}\int_{-1}^{1} d\alpha \int_{-\sqrt{1-\alpha^2}}^{\sqrt{1-\alpha^2}} d\beta \left(A^2\,|X(\alpha,\beta)|^2 \frac{(\lambda^2+\mu^2)}{(1-\alpha^2-\beta^2)^{1/2}}\right) \quad (22)$$

In order to predict the radiation efficiency in a frequency band under force excitation, a modal summation approach can be adopted. The modal amplitudes due to a unit force are calculated using the usual expression:

$$v_{pq} = \frac{4j\omega}{m(\omega_{pq}{}^2(1+j\eta)-\omega^2)}\sin\left(\frac{p\pi x_0}{a}\right)\sin\left(\frac{q\pi y_0}{b}\right) \quad (23)$$

where the force is applied at the position (x_0, y_0), η is the loss factor and m is the mass of the plate. By taking an average over all possible forcing locations the sine terms can be eliminated. Finally the overall radiated power at each frequency is found from

$$W = \sum_{p,q} W_{pq} = \rho_0 c(ab)\sigma_{pq}\frac{|v_{pq}|^2}{8} \quad (24)$$

4 EXPERIMENTAL RESULTS FOR UNBAFFLED PLATES

To the best of the authors' knowledge, the only experimental investigations of sound radiation by vibrating perforated plates have been applied to unbaffled plates[4,5,6]. In this section the results of these investigations are compared with predictions from the previous section. Although the radiation efficiencies of unbaffled plates differ from those in the presence of a baffle, by presenting the results as insertion losses, this effect is minimised. Whilst these results can be expected to differ from the theory of the previous section at low frequencies, it is anticipated that the theory may give a

reasonable approximation at higher frequencies. It should be pointed out that such measurements involve the combination of two measurements (spatially averaged velocity and radiated power) to obtain the radiation efficiency, and the combination of two radiation efficiencies to obtain the insertion loss. The potential for experimental error is therefore quite large.

In the first set of experiments by Pierri[4] (see also ref. 3) the radiation efficiency of a series of square steel plates of dimensions 0.3x0.3 m and thickness 1.22 mm was measured. These had perforation ratios (ratio of perforated area to total plate area) between 6% and 42% and were freely suspended. The equivalent unperforated plate was also measured. The plates were excited using a shaker and the spatially averaged squared velocity was determined using an accelerometer. An average of three force positions was used. Then the sound power was measured in a reverberation room.

These results are plotted in Figure 3 in the form of the effect of perforation on the radiation ratio. Also shown in the figure is the result of predicting the insertion loss using the model of the previous section. Generally very good agreement is seen above about 1 kHz, where the model gives a correct distinction between the different cases. The results (measured and predicted) at frequencies above 1 kHz have a frequency dependence of approximately 10 dB per decade. At low frequencies, well below the critical frequency, the prediction is affected more by the presence of the (perforated) baffle. The measurements appear to tend towards a constant value at low frequencies, whereas the predicted results fall at about 20 dB per decade (similar to Figure 2). It is also possible that the measured results were affected by shaker noise at low frequencies.

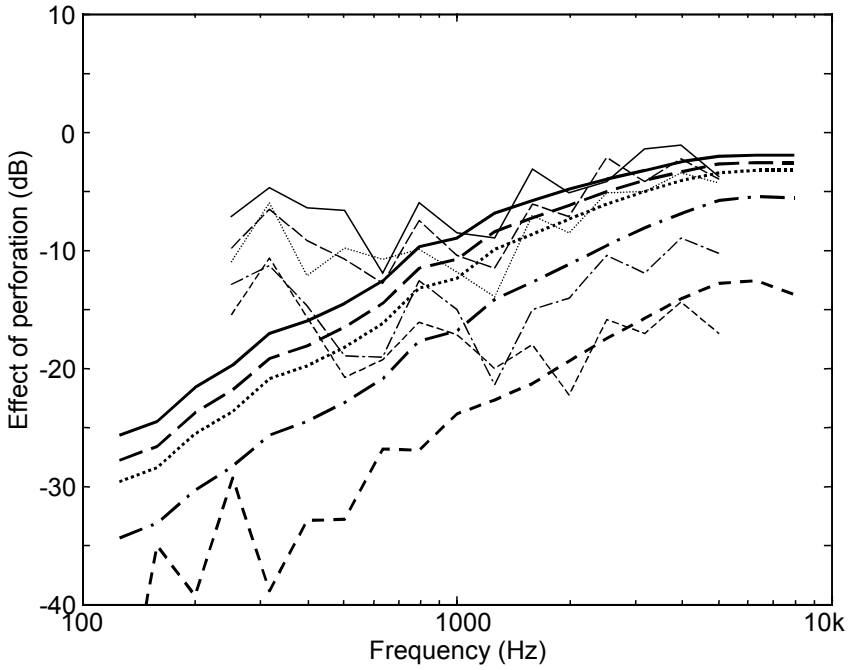

Figure 3. Effect of perforation on radiation ratio of 1.22 mm steel plates 0.3x0.3 m, critical frequency 10 kHz. — 5.6 mm diameter holes, 6% perforation, – – – 7.2 mm diameter, 9% perforation, ····· 8.8 mm diameter, 14% perforation, – · – · 15 mm diameter, 42% perforation, - - - 3.2 mm diameter, 37% perforation. Thin lines: experiments[4], thick lines predicted.

A recent experiment[6] has used a scanning laser vibrometer to measure the plate vibration, and a reciprocal method to measure the radiation efficiency in a reverberation room. The plates were 3 mm thick aluminium of dimensions 0.4x0.3 m and were suspended freely. The perforation patterns considered included several different hole sizes corresponding to the same perforation ratio. The results are shown in Figure 4. Here, as in Figure 3, good agreement is found above about 1 kHz, including above the critical frequency of 4 kHz in the present case.

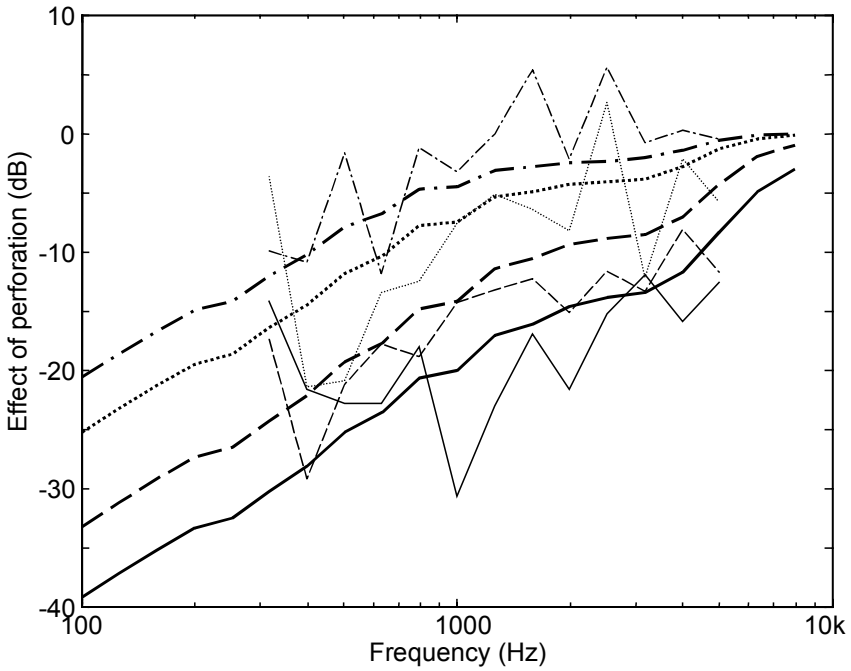

Figure 4. Effect of perforation on radiation ratio of 3 mm aluminium plates 0.4x0.3 m, critical frequency 4 kHz. — 5 mm diameter holes, 20% perforation, – – – 10 mm diameter, 20% perforation, ····· 25 mm diameter, 20% perforation, – · – · 15 mm diameter, 7% perforation. Thin lines: experiments[6], thick lines predicted.

There are several differences between the model and the experiments: the model is of a plate mounted in a perforated baffle while the measurements are of unbaffled plates, the model uses simply supported plate modes whereas the measurements in two cases are of free-free modes. Nevertheless, there is good agreement at the higher frequencies in terms of insertion loss indicating that the model can be used for engineering design.

The results in Figure 3 indicate that, as expected, the sound radiation is reduced as the perforation ratio is increased. However, the results in Figure 4 show that the sound radiation is also reduced as the hole size is reduced for a given perforation ratio. This is seen from the parameter h (Eq. (2)), since, for thin plates ($t << r$) the perforation ratio γ is equal to $\pi r^2/S$ so that $h = \pi kr/2\gamma$. Thus a given value of h can be achieved by small holes and a small perforation ratio, or by larger holes and a corresponding larger perforation ratio.

5 SOUND RADIATION BY A UNIFORMLY VIBRATING PERFORATED STRIP SET IN A PERFORATED BAFFLE

In practice, perforated plates are not usually set in similarly perforated baffles. As explained in the Introduction, the general three-dimensional model of a perforated rectangular plate set in a *rigid* baffle is computationally extremely intensive. The same applies to the unbaffled perforated plate. As an interim exploration of the influence of baffle impedance on the sound radiation by vibrating perforated surfaces, the following analysis is restricted to the two-dimensional case. An infinitely long, rigid, perforated piston of finite width is assumed to be vibrating within a coplanar perforated baffle of arbitrary specific acoustic impedance, Figure 5.

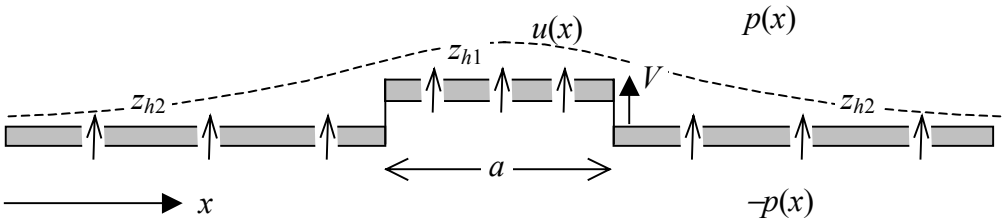

Figure 5. A perforated strip of width a set in an infinite perforated plate of different impedance.

A strip piston of width a vibrates at frequency ω with spatially uniform velocity amplitude V. The magnitudes of the specific acoustic impedances associated with the perforation of the piston and baffle are denoted by z_{h1} and z_{h2}, respectively. The relation between pressure on the upper surface and the equivalent continuously distributed fluid velocities through the piston and the baffle are

$$u(x) = -2\frac{p(x)}{z_{h1}} \quad \text{on } -a/2 < x < a/2 \quad \text{and} \quad u(x) = -2\frac{p(x)}{z_{h2}} \quad \text{on } x < -a/2 \text{ or } x > a/2 \qquad (25a,b)$$

The pressure distribution $p(x)$ is expressed in terms of the Inverse FT of its wavenumber spectrum $p(k_x)$ as

$$p(x) = \frac{1}{2\pi}\int_{-\infty}^{\infty} p(k_x)\exp(jk_x x)dk_x \qquad (26)$$

Now, $p(k_x)$ is related to the sum of the spectral components of the piston velocity and the flow through the piston and baffle by

$$p(k_x) = w(k_x)z_a(k_x) = \big(v(k_x) + u(k_x)\big)z_a(k_x) \qquad (27)$$

Hence

$$u(x) = -\frac{1}{\pi z_{h1}}\int_{-\infty}^{\infty} z_a(k_x)[v(k_x) + u(k_x)]\exp(jk_x x)dk_x \quad \text{on } -a/2 < x < a/2 \qquad (28)$$

$$u(x) = -\frac{1}{\pi z_{h2}}\int_{-\infty}^{\infty} z_a(k_x)[v(k_x) + u(k_x)]\exp(jk_x x)dk_x \quad \text{on } x < -a/2 \text{ or } x > a/2 \qquad (29)$$

The spectral components of the distributions of velocity u are given by the FT of $u(x)$ as

$$\begin{aligned} u(k_x') = &-\frac{1}{\pi z_{h1}}\int_{-\infty}^{\infty} dk_x \int_{-a/2}^{a/2} z_a(k_x)[v(k_x) + u(k_x)]\exp(jk_x x - jk_x' x)dx \\ &-\frac{1}{\pi z_{h2}}\int_{-\infty}^{\infty} dk_x \int_{-\infty}^{-a/2} z_a(k_x)[v(k_x) + u(k_x)]\exp(jk_x x - jk_x' x)dx \\ &-\frac{1}{\pi z_{h2}}\int_{-\infty}^{\infty} dk_x \int_{a/2}^{\infty} z_a(k_x)[v(k_x) + u(k_x)]\exp(jk_x x - jk_x' x)dx \end{aligned} \qquad (30)$$

The integration intervals in the second and third line of Eq.(30) may be rewritten as

$$\int_{-\infty}^{-a/2} + \int_{a/2}^{\infty} = \int_{-\infty}^{\infty} - \int_{-a/2}^{a/2}$$

The infinite integral simply forms a FT pair, leaving

$$u(k_x') = \left(\frac{1}{\pi z_{h2}} - \frac{1}{\pi z_{h1}}\right)\int_{-\infty}^{\infty} dk_x \int_{-a/2}^{a/2} z_a(k_x)[v(k_x)+u(k_x)]\exp(jk_x x - jk_x' x)dx - \frac{2z_a(k_x')}{z_{h2}}[v(k_x')+u(k_x')] \tag{31}$$

which gives

$$u(k_x')\left[1+\frac{2z_a(k_x')}{z_{h2}}\right] + v(k_x')\frac{2z_a(k_x')}{z_{h2}} = \frac{a}{\pi}\left(\frac{1}{z_{h2}} - \frac{1}{z_{h1}}\right)\int_{-\infty}^{\infty} dk_x z_a(k_x)[v(k_x)+u(k_x)]\mathrm{sinc}([k_x - k_x']a/2) \tag{32}$$

where $\mathrm{sinc}(f) = \sin(f)/f$ and the spectrum of velocity of the strip piston is $v(k_x) = Va\mathrm{sinc}(k_x a/2)$. The interpretation of the presence of the sinc function in Eq.(32) is that a discontinuity of perforate impedance at the edges of the piston creates a 'window' effect that 'couples' different wavenumber spectral components.

This equation was solved numerically for $u(k_x)/v(k_x)$ by selecting a finite range for k_x and an interval δk_x and approximating the integral by a sum over the discrete values of k_x. This results in a set of linear algebraic equations which are expressed in terms of vectors and matrices and solved by matrix inversion in a Matlab program. This procedure is similar to that used in the Boundary Element Method except that here it is formulated in the wavenumber domain. The poles of $z_a(k_x)$ at $k = \pm k_x$ were handled by an analytic approximation.

Once the ratio $u(k_x)/v(k_x)$ is found for all selected values of k_x, the radiated sound power per unit length of the piston is found by evaluation of the sum over all selected k_x within the range $-k$ to $+k$ of the expression

$$W' = \sum_{-k<k_x<k} W'(k_x) = \frac{\delta k_x}{4\pi}\sum_{-k<k_x<k} z_a(k_x)|v(k_x)|^2\,\mathrm{Re}\left\{1+\frac{u(k_x)}{v(k_x)}\right\} \tag{33}$$

The corresponding radiation efficiency is given by $\sigma = 2W'/\rho_0 caV^2$.

It may be deduced from the discretized version of Eq.(32) that the solution for each discrete value of $u(k_x)/v(k_x)$ is a function of the non-dimensional specific impedance ratios $z_a(k_x)/z_{h1}$ and $z_a(k_x)/z_{h2}$ and of the value of $[(1/z_{h2}) - (1/z_{h1})]$. When the piston and the baffle are identically perforated, the latter is zero, the 'window' effect is not present, and the solution corresponds to that given by Eq.(11). Otherwise, the smaller of the two perforate impedances is a controlling factor. The unbaffled state may be approximated by means of the artifice of making $|z_{h2}|/\rho_0 c << 1$. A rigid baffle is represented by making $|z_{h2}|$ infinite (or very large).

Figure 6 shows the predicted radiation ratio for a strip in a near-rigid baffle (very large z_{h2}). At low ka the result for the unperforated strip is proportional to ka (approximately equal to $ka/2$) The results for different values of h show a slope of $(ka)^2$ at moderately high ka (as in Figure 2), but this reduces to a slope proportional to ka at low ka. These results were produced for a = 0.3 m and h/k = 0.64, 0.16, 0.04 and 0.01. However, it is found that, if a is varied, identical results are obtained provided that h/ka is kept constant.

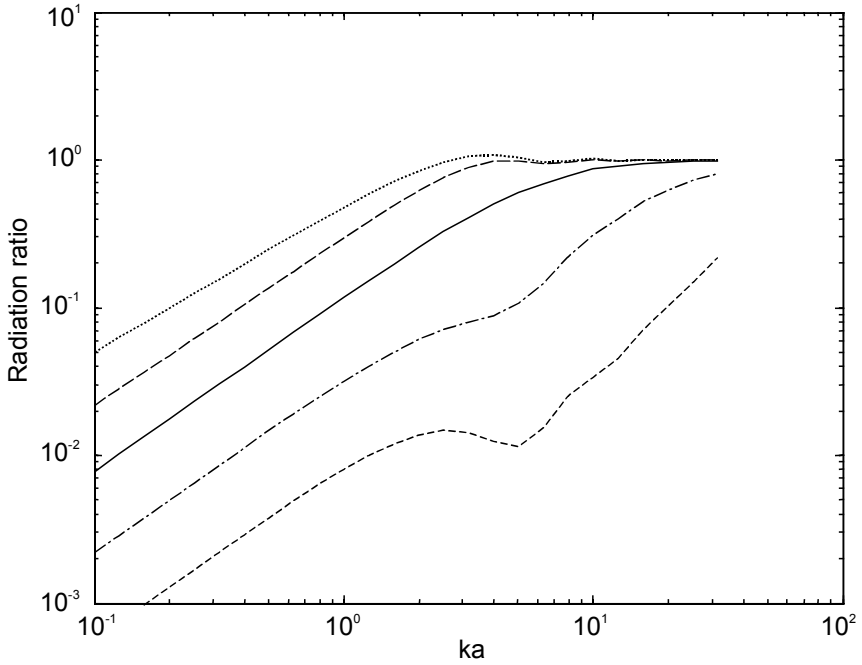

Figure 6. Radiation ratio of a strip-piston in a rigid baffle. ····· unperforated, – – – h/ka = 2.13, — h/ka = 0.53, – · – · h/ka = 0.13, - - - h/ka = 0.033.

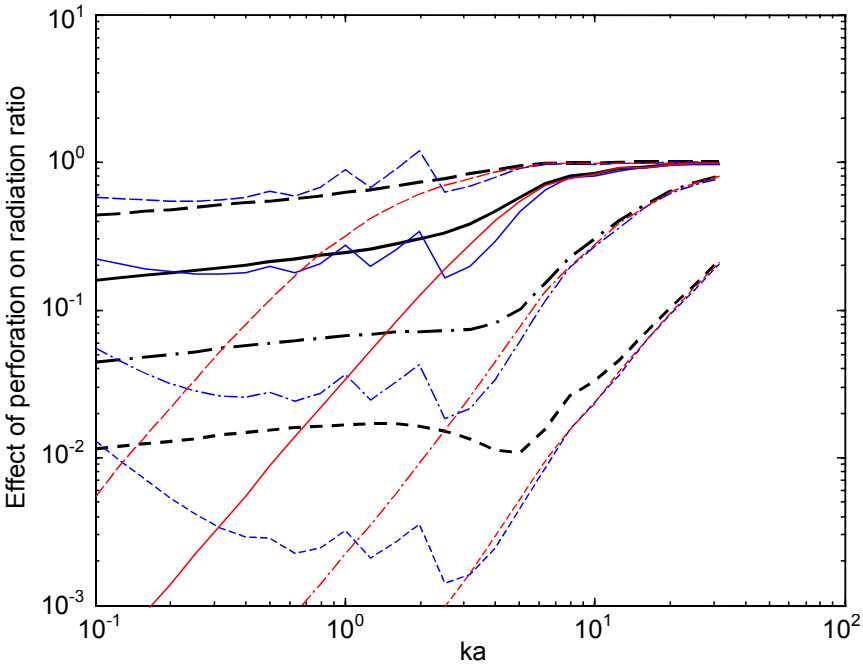

Figure 7. Effect of perforation on the radiation ratio of a strip-piston in a rigid baffle (thick lines), in a low impedance baffle (thin blue lines) and in a perforated baffle (thin red lines) for different h/ka: – – – 2.13, — 0.53, – · – · 0.13, - - - 0.033.

The effect of perforation is shown in Figure 7 as the ratio of σ for the perforated case to σ for the unperforated case. Also shown are results for a baffle with very low impedance (very small z_{h2}) and for a perforated baffle ($z_{h2} = z_{h1}$). These show that, although the radiation ratios of baffled and unbaffled plates differ, the effect of perforation is similar in each case. For the perforated baffle, the

effect is similar to that for the unbaffled case for $ka > 2$, but much greater at low ka. For a rigid baffle the effect of perforation tends to a constant value at low ka that depends on h/ka. The dependence on h/ka is shown explicitly in Figure 8 for ka = 0.1 and 1. For the plates of Pierri (Figure 3) h/ka is between 0.26 and 0.023 which correspond to a constant effect between –9.5 and –20.1 dB at low frequency. This helps to explain the low frequency trends seen in Figure 3.

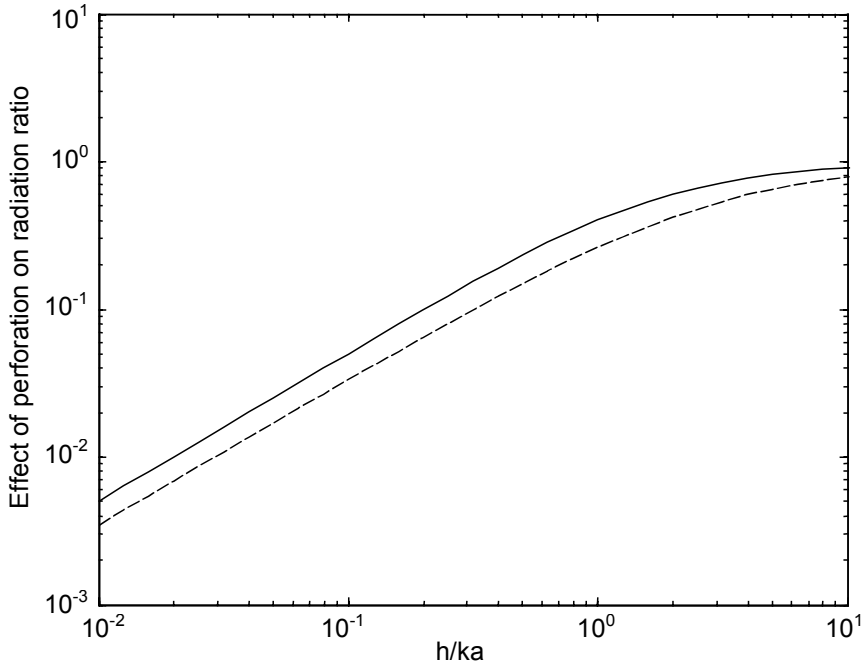

Figure 8. Effect of perforation on radiation ratio of a strip-piston in a rigid baffle. – – – ka = 0.1, — ka = 1.

6 CONCLUDING REMARKS

A model for the sound radiation from perforated plates has been developed. By assuming that the plate is set in an infinite baffle that is similarly perforated, the numerical evaluation is made considerably easier. Comparisons are made with measured results on unbaffled plates from different sources. Reasonable agreement is found at moderately high frequencies. At low frequencies, however, the influence of the lack of a baffle must be taken into account. This has so far been done only for a one-dimensional strip piston, but from this it is seen that it is possible to use the method to approximate radiation from both baffled and unbaffled plates. Development of the full two-dimensional model is continuing, although it is recognised that it is computationally extremely intensive. It has been shown that the insertion loss due to perforation increases as either the proportion of the area that is perforated increases or the hole size decreases.

7 REFERENCES

1. A. D. Pierce. Acoustics, Acoustical Society of America (1989).
2. S. N. Rschevkin. A Course of Lectures in the Theory of Sound, Pergamon (1963).
3. F. J. Fahy. Sound and Structural Vibration, Academic Press (1987).
4. R. A. Pierri. Study of a dynamic absorber for reducing the vibration and noise radiation of plate-like structures. MSc Dissertation, ISVR, University of Southampton (1977).
5. M.H.A. Janssens, W.J. van Vliet, Noise from steel bridges: research into the effect of perforations of bridge components (in Dutch). TNO report TPD-HAG-RPT-960057 (1996).
6. L. Robertson, Determination of the radiation efficiency of perforated plates. BEng project report, ISVR, University of Southampton (2003).